Spectrochimica Acta Part B 64 (2009) 369–377

Contents lists available at ScienceDirect

Spectrochimica Acta Part B

journal homepage: www.elsevier.com/locate/sab

Evaluation of laser induced breakdown spectroscopy for the determination of micronutrients in plant materials

Lilian Cristina Trevizan [a], Dário Santos Jr. [b], Ricardo Elgul Samad [c], Nilson Dias Vieira Jr. [c], Lidiane Cristina Nunes [a,d], Iolanda Aparecida Rufini [a], Francisco José Krug [a,*]

[a] Centro de Energia Nuclear na Agricultura-Universidade de São Paulo, Av. Centenário 303, 13416-000, Piracicaba-SP, Brazil
[b] Universidade Federal de São Paulo - UNIFESP, Rua Prof. Artur Riedel 275, 09972-270, Diadema-SP, Brazil
[c] Centro de Lasers e Aplicações, IPEN/CNEN-SP, Av. Prof. Lineu Prestes 2242, 05508-000, São Paulo-SP, Brazil
[d] Departamento de Química, Universidade Federal de São Carlos, Rodovia Washington Luís (SP-310), km 235, 13565-905, São Carlos-SP, Brazil

ARTICLE INFO

Article history:
Received 25 September 2008
Accepted 6 April 2009
Available online 17 April 2009

Keywords:
LIBS
Plant material
Micronutrients
Laser-induced breakdown spectrometry

ABSTRACT

Laser induced breakdown spectroscopy (LIBS) has been evaluated for the determination of micronutrients (B, Cu, Fe, Mn and Zn) in pellets of plant materials, using NIST, BCR and GBW biological certified reference materials for analytical calibration. Pellets of approximately 2 mm thick and 15 mm diameter were prepared by transferring 0.5 g of powdered material to a 15 mm die set and applying 8.0 tons cm^{-2}. An experimental setup was designed by using a Nd:YAG laser operating at 1064 nm (200 mJ per pulse, 10 Hz) and an Echelle spectrometer with ICCD detector. Repeatability precision varied from 4 to 30% from measurements obtained in 10 different positions (8 laser shots per test portion) in the same sample pellet. Limits of detection were appropriate for routine analysis of plant materials and were 2.2 mg kg^{-1} B, 3.0 mg kg^{-1} Cu, 3.6 mg kg^{-1} Fe, 1.8 mg kg^{-1} Mn and 1.2 mg kg^{-1} Zn. Analysis of different plant samples were carried out by LIBS and results were compared with those obtained by ICP OES after wet acid decomposition.

1. Introduction

The determination of essential elements in plant materials is of key importance to evaluate the nutritional status of crops of economical interest. From the knowledge of the concentration of the most important nutrients in the plant leaves, one can define the best strategy to correct any deficiency, if present, that will limit the production and/or the quality of fruits, vegetables, and cereals, for example. Essential macronutrients (N, P, K, Ca, Mg, S) and essential micronutrients (Fe, Cu, Mn, Zn, B, Mo, Cl and Ni) play a decisive role in plant nutrition and can affect crop yields when they are not present in appropriate concentration levels [1]. In general, to evaluate the crop nutritional status, the laboratory samples are washed, dried and ground and further steps of the analytical sequence include a wet acid digestion of a given test portion (250–1000 mg) in open or closed systems, prior to the determination. The most recommended technique for large routine analysis of acid digests is ICP OES, due to its inherent multielement and simultaneous analytical capabilities for almost all macro and micronutrients that may limit plant growth and productivity. For instance, accurate determinations of P, K, Ca, Mg, S, Fe, Cu, Mn, Zn and B can be carried out in approximately 20–30 s in each digest in modern instrumentation with radial or axial viewing ICP. The determination of Mo can be carried out by graphite furnace atomic absorption spectrometry, but is not often determined, in spite of its importance, because it occurs in low concentrations. Chloride deficiencies are very rare and not observed in plants of economical interest, and the determination of this essential element is very rare and/or not relevant. The remaining micronutrient, which is not included in routine analysis, is nickel, mainly because its deficiency was not yet observed in higher plants. On the other hand, nickel toxicity may limit plant growth. Other important elements that are not essential but may present beneficial effects to plant development are Co, Na and Si [1].

Taking into consideration the scope of this paper, the general range of concentrations of micronutrients for most plants of agricultural interest in good nutritional status is assumed to be 10–200 mg kg^{-1} B, 3–50 mg kg^{-1} Cu, 50–900 mg kg^{-1} Fe, 20–2000 mg kg^{-1} Mn and 5–200 mg kg^{-1} Zn on dry matter basis [2].

Most recently, we started a project in Brazil for overcoming the main drawbacks towards clean chemistry, trying to avoid acid digestion procedures, which also requires appropriate exhaustion fume hoods as well as additional on line treatment of emitted toxic gases. Direct solid analysis of agricultural and environmental samples by laser induced breakdown spectroscopy (LIBS) was chosen as the alternative technique to be evaluated for the simultaneous multi-elemental determinations of the most important essential and beneficial elements in plant materials.

In this sense, an evaluation of LIBS for the determination of P, K, Ca and Mg in pellets of plant materials was carried out in our laboratory [3]. A LIBS system equipped with a 360 mJ/pulse Nd:YAG laser at 1064 nm was used and calibration was done with certified reference

* Corresponding author. Fax: +55 19 34294610.
E-mail address: fjkrug@cena.usp.br (F.J. Krug).

0584-8547/$ – see front matter © 2009 Elsevier B.V. All rights reserved.
doi:10.1016/j.sab.2009.04.003

materials (CRMs). Results compared reasonably with data obtained by ICP OES, but the coefficients of variation of LIBS results were somewhat high (5–25%), and were attributed to analyte micro-heterogeneity in the sample pellet.

The biological applications of LIBS reported in the literature are still limited to a few applications, such as the determination of trace elements in teeth [4], minerals and potentially toxic elements in calcified tissue [5], Zn in human skin [6], Ca in sunflower seedling stem [7], elements in human hair [8] and trace elements in malignant tissue cells [9]. In addition, detection and identification of bacteria [10] and a study of the process of tissue ablation of collagen gels and porcine cornea with ultrashort laser pulses [11] were also reported. Samek et al. [12] used a femtosecond laser for the determination of Fe in leaves vein and parts of leaf positioned between the veins. In another paper, LIBS method capable of mapping Cd and Pb in biological structures, that accumulate metals in leaves and roots, was proposed and data compared well with X-ray microradiography [13]. Galiová et al. [14] showed the spatial resolution mapping of Pb in plant leaves and results suggested that elevated levels of this analyte influence the concentration and distribution of K and Mn within the sample. LIBS qualitative analysis of fresh vegetables were performed by Juvé et al. [15] using an ultraviolet nanosecond laser. Trace elements were identified in the LIBS spectra and space-resolved analysis has been performed in roots, stems and fruits due to the high spatial resolution of the technique. The application of LIBS for fast analysis of large areas of sunflower leaves and mapping of Pb, Mg and Cu accumulation was evaluated by Kaiser et al. [16].

Most recently fs-LIBS was evaluated for the determination of Ca, Cu, Fe, K, Mg, Na and P [17] and it was concluded that the LIBS method proposed is useful for the development of quantitative methods for analysis of animal tissues. However, the optimal experimental parameters for fs-LIBS implementation have not yet been found, and, consequently, there is a large need for methodical experimental optimization.

At our best knowledge, there is only one paper dealing with a method for direct solid analysis of plant leaves by LIBS [18] aiming the determination of some micronutrients (Fe, Cu, Mn, and Zn) as well as macronutrients (P, Ca, and Mg). The powdered leaf sample was applied directly on a double-sided tape on a glass slide and a 100 mJ/pulse Nd:YAG laser at 1064 nm was used to form the laser induced plasma. Calibration curves were made with certified reference materials (CRMs) and trueness for Mn and Zn was checked against data obtained by ICP OES from a Spanish moss acid extract obtained with 1 mol l^{-1} HNO_3. There was no information for Cu and Fe.

The aim of this work is to show preliminary results on the determination of micronutrients (B, Cu, Fe, Mn and Zn) in pellets of powdered samples by using a ns-LIBS system with a simple ablation chamber designed for routine analysis. Certified reference materials from NIST, BCR, GBW and reference materials from IAEA were used for calibration and accuracy was evaluated by using CRMs not employed in the calibration or by comparison of results from the analysis of plant samples by ICP OES after wet acid decomposition.

2. Experimental

2.1. LIBS instrumentation

A Q-switched Nd:YAG laser (Brilliant, Quantel, France) operating at the fundamental wavelength (1064 nm) was employed. Laser pulses with (365 ± 3) mJ, 5 ns (FWHM) at 10 Hz repetition rate were generated with a 6 mm diameter beam quality factor M^2 smaller than 2. The laser pulse was focused on the sample pellet by a convergent lens with 2.54 cm diameter and 20 cm focal length (Edmund Optics, USA). The lens-to-sample distance (LTSD) was kept shorter than the lens focal length so that most of the laser energy was deposited into the material bulk. In this situation, the LTSD and the pulse energy were adjusted at 16.5 cm and 200 mJ, respectively, as recommended [3].

The 15 mm diameter pellet was placed into a plastic sample holder in a two axes manual controlled translation stage that moved in the plane orthogonal to the laser direction. Argon flowing at 0.5 l min^{-1} was continuously fed into the ablation chamber by two entrance inlets symmetrically positioned in the sample holder and the flow-rate was controlled by a rotameter. The plasma emission was colleted by a telescope composed of 50 mm and 125 mm focal length fused silica lenses (Edmund Optics, USA), and the collected light was injected into the spectrometer fiber (1.5 m, 600 μm core) matching its numerical aperture. The optical axis of the collecting system was approximately 25° from the laser axis.

A model ESA 3000 spectrometer (LLA Instruments GmbH, Germany) equipped with echelle optics and focal length of 25 cm with numerical aperture of 1:10 was used, which provides a 24.5 × 24.5 mm^2 flat image plane. This system is a compromise that offers maximum resolution in the wavelength range of 200 to 780 nm with resolving power ranging from 10,000 to 20,000. The linear dispersion per pixel ranges from 5 pm at 200 nm to 19 pm at 780 nm. The wavelength calibration was checked by using Hg and Zn atomic lines from electrodeless discharge lamps (EDL II System, Perkin Elmer, Germany). The detector is an ICCD camera, comprised of a Kodak KAF 1001 CCD array of 1024 × 1024 pixels full frame (24 × 24 μm^2) and a microchannel plate image intensifier of 25 mm diameter coupled to a UV-enhanced photocathode. The image signals are digitalized in dynamic range of 16 bits and further processed by an industrial computer. The dark current of the ICCD was automatically subtracted from the measured spectral data. The integration time gate and the number of pulses accumulated were fixed at 5 μs and 8 pulses, respectively, for all measurements presented in this work, except otherwise mentioned. The delay time was evaluated and the temporal history of the plasma was obtained by recording the emission intensity of plasma at predetermined delay times.

2.2. Samples and reference materials

Bean leaves (*Phaseolus vulgaris*) were chosen to perform preliminary experiments and for the estimation of plasma temperature

Table 1
Characteristics and operational parameters of axially viewed ICP OES used for analysis of plant wet acid digests.

Characteristics	Vista AX ICP OES
Generator frequency	40 MHz
Detector	Peltier cooled CCD
	70,908 pixels spread across 70 non-linear arrays
	Wavelength range = 167–785 nm
Torch internal tube diameter	2.3 mm
Optical system	
Polychromator	Echelle-grating + CaF_2 cross dispersing prism
Grating density groove	95 grooves mm^{-1}
Focal length	400 mm
Entrance slit	Height = 0.029 mm and width = 0.051 mm
Sample introduction system	
Nebulizer	V-groove
Spray chamber	Sturman-Masters
Operational parameters	
RF power	1.2 kW
Plasma gas flow-rate	15.0 l min^{-1}
Auxiliary gas flow-rate	1.5 l min^{-1}
Nebulizer gas flow-rate	0.9 l min^{-1}
Sample flow-rate	0.8 ml min^{-1}
Emission lines	B I 249.771 nm
	Cu I 327.395 nm
	Fe II 259.940 nm
	Mn II 257.610 nm
	Zn II 206.200 nm

and temporal characterization. The leaves were washed separately with running tap water and further rinsed twice with distilled water and three times with ultra purity water. After washing, samples were dried, chopped and oven-dried to constant mass at 60 °C during 48–96 h. Leaves were ground and homogenized by using a cryogenic mill model MA-775 (Marconi) with a self-container liquid nitrogen bath. A pre-cooling time of 5 min was used with further 2 min grinding.

The following certified reference materials and reference materials were used for calibration: aquatic plant (Community Bureau of Reference — BCR 60), aquatic moss (BCR 61), olive leaves (BCR 62), bush branches and leaves (National Research Centre for CRM's — GBW 07603), cabbage (International Atomic Energy Agency — IAEA 359), rice flour (National Institute for Environmental Studies — NIES 10-c), apple leaves (National Institute of Standards and Technology — NIST 1515), peach leaves (NIST 1547), wheat flour (NIST 1567a) and spinach leaves (NIST 1570a). The following materials were homogenized by cryogenic grinding prior to sample pellet preparation: BCR 61, GBW 07603 and NIES 10-c.

Pellets were prepared in a Spex model 3624B X-Press by transferring 0.5 g of powdered material to a 15 mm die set and applying 8.0 tons cm^{-2} during 10 min. Pellets were approximately 2 mm thick and 15 mm diameter. At least ten spectra of each sample were collected in 10 different test portions of the pellet. Each test portion was the mass removed from the pellet after 8 laser shots.

For comparison of LIBS and ICP OES results, different plant samples were decomposed with nitric and perchloric acids using a block digestor (Marconi, Piracicaba, Brazil). Samples were decomposed in triplicate in open digestion tubes according to the following procedure: 500 mg of dried and ground sample was kept overnight (approximately 12 h) with 5.0 ml of 14 mol l^{-1} HNO_3 at room temperature in a fume hood. The mixture was then digested at a block digestor temperature not exceeding 160 °C for approximately 3 h.

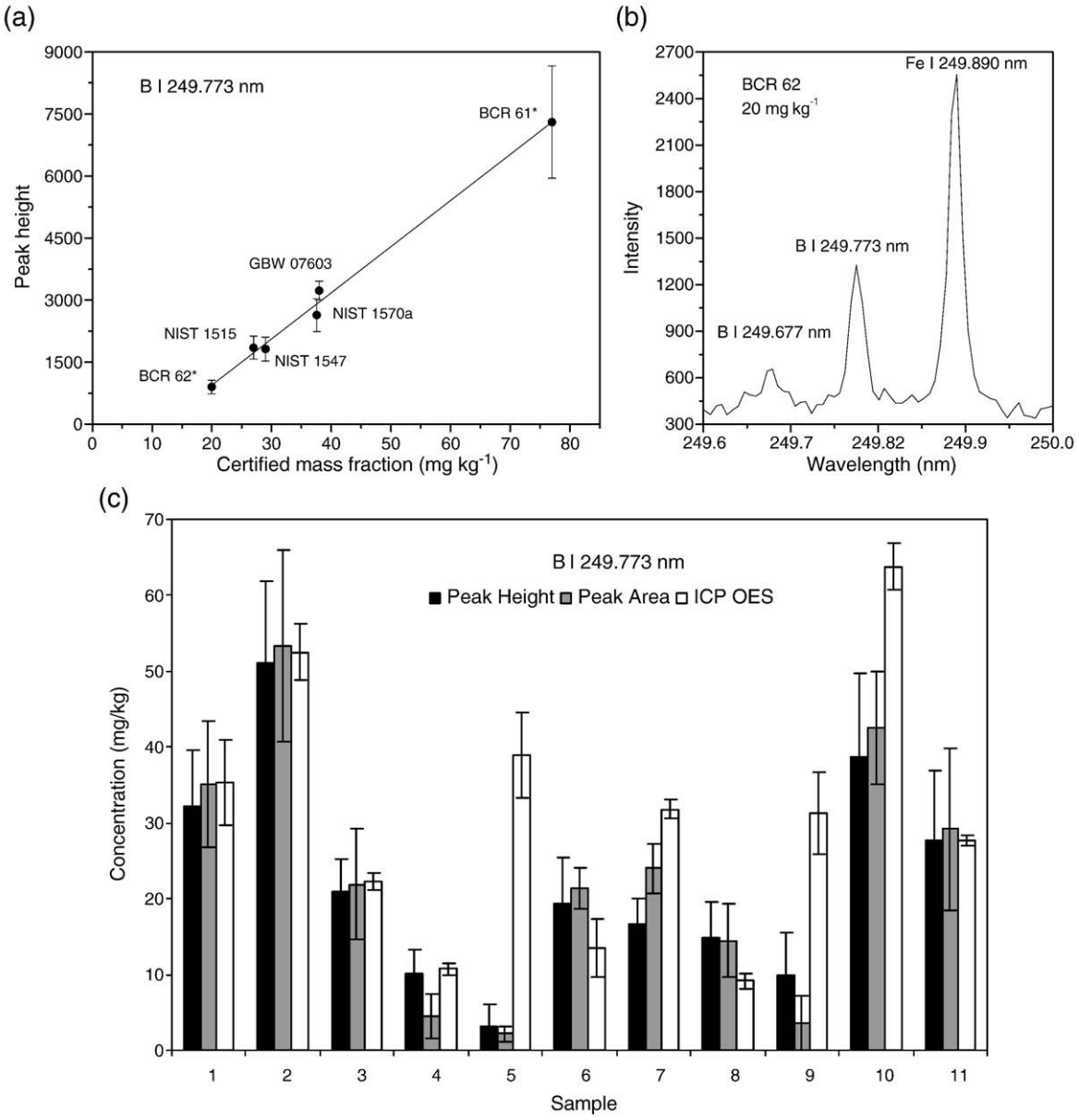

Fig. 1. (a) Analytical calibration curve for B I 249.773 nm using reference materials. (b) Signal profiles for B I at 249.677 and 249.773 nm. (c) LIBS concentrations of B in plant samples calculated with peak height and peak area compared to ICP OES results. Leave samples: 1 - lettuce (*Lactuca sativa*), 2 - endive (*Cichorium endivia*), 3 - boldo (*Pneumus boldus*), 4 - brachiaria (*Brachiaria decumbens*), 5 - coffee (*Coffea arabica*), 6 - grass (*Axonopus obtusifolius*) , 7 - jack (*Artocarpus integrifolia*), 8 - mango (*Mangifera indica*), 9 - maize (*Zea mays*), 10 - pepper (*Piper nigrum*), 11 - soya (*Glycine max*). *Non-certified mass fraction. Uncertainty bars correspond to one estimated standard deviation ($n = 10$, 8 pulses per test portion).

After cooling, the excess of nitric acid was driven off by adding 1.3 ml 72% $HClO_4$ and increasing the block digestor temperature to 210 °C. Heating was continued until a clear colorless solution was obtained and dense fumes of perchloric acid dihydrate appears. After cooling, the digests were diluted with water up to 50 ml and analysed by axially viewed ICP OES (Vista AX, Varian, Australia) with the operational parameters showed in Table 1.

3. Results

The temperature of the induced micro-plasma in pellets of plant materials was estimated through Boltzmann plots by using Fe(I) lines and varied between 10,140 and 7720 K at the delay times from 1 to 4 μs, respectively [3]. At 2 μs the plasma excitation temperature was 9130 ± 130 K. Gate delay time and integration time was fixed at 2 and 5 μs, respectively, due to a better signal-to-noise ratio obtained at these conditions. The LIBS spectrum obtained under argon atmosphere (0.5 l min^{-1} Ar flow-rate) was significantly more intense than in the presence of air. Similar results were previously reported in the literature [19].

Pellets of reference materials were analyzed by the proposed LIBS system by applying 8 consecutive laser shots in 10 different positions (test portions) at the sample surface and data was based on cumulative spectra. The lens-to-sample distance was kept at 16.5 cm. For calibration, most data refers to certified mass fractions, but a reference material (IAEA 359) was also used for some analytes. By keeping the same strategy done for evaluation of macronutrients [3], it was decided to use the CRMs even knowing that there was a recommendation in the certificates stating that the certified values were based on a minimum sample mass of 150 mg. The calculated mass of the 10 ablated test portions with 8 pulses each was approximately 360 μg.

Figs. 1–5 show the analytical calibration curves of B, Cu, Fe, Mn and Zn, a selected peak profile of each analyte in the selected wavelength and LIBS results from the analysis of 11 pellets of plant samples compared to the analysis of the corresponding acid digests by ICP OES. All data was based on background corrected peak height and/or peak areas. The calculated coefficient of variations of peak height intensities for each reference material used in the analytical calibration curves varied from 4 to 30% ($n = 10$). In spite of previous assumptions [3,17]

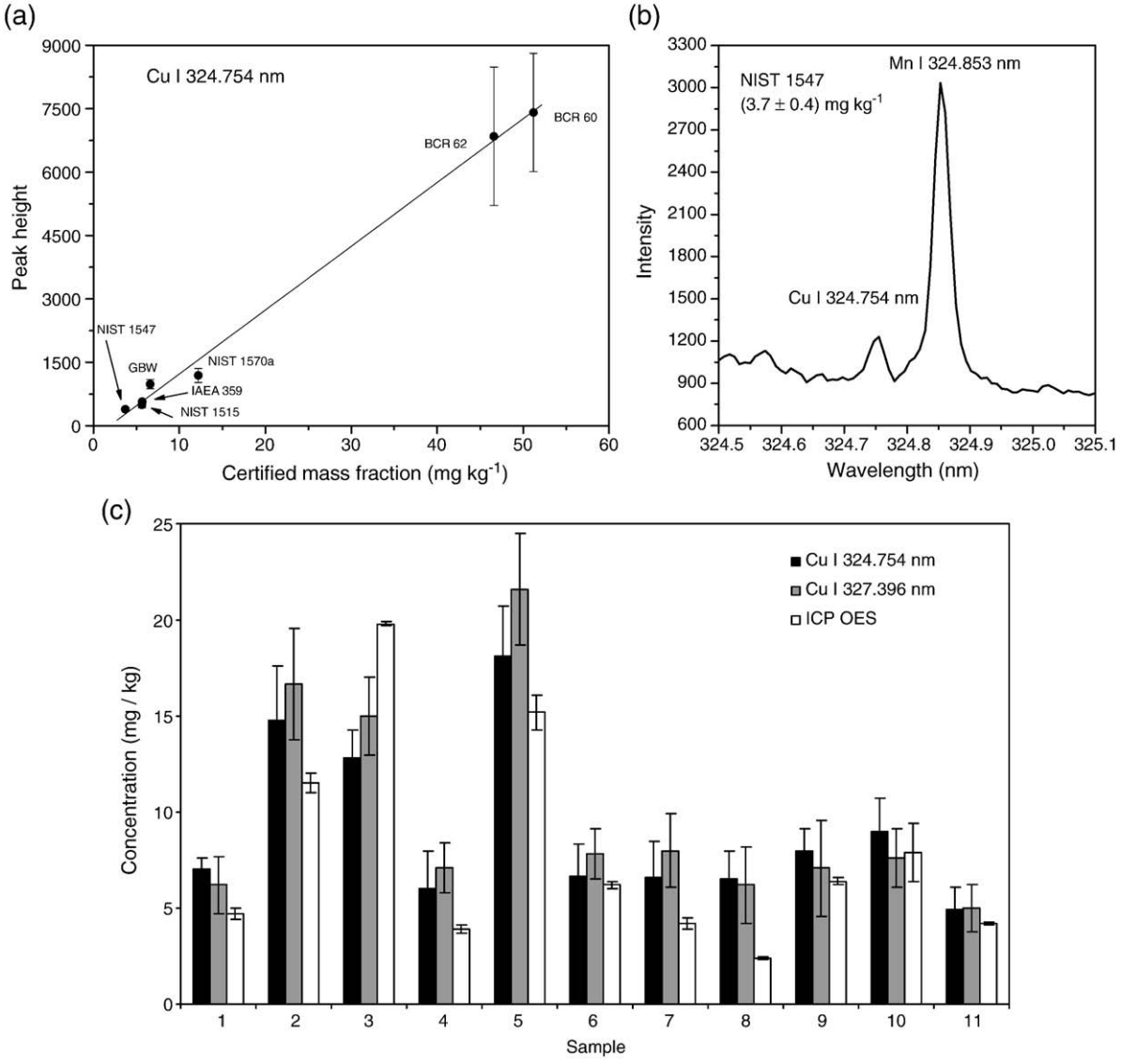

Fig. 2. (a) Analytical calibration curve for Cu I 324.754 nm. (b) Signal profile for Cu I. (c) LIBS concentrations of Cu in plant samples compared to ICP OES results. Leave samples: 1 - lettuce (*Lactuca sativa*), 2 - endive (*Cichorium endivia*), 3 - boldo (*Pneumus boldus*), 4 - brachiaria (*Brachiaria decumbens*), 5 - coffee (*Coffea arabica*), 6 - grass (*Axonopus obtusifolius*), 7 - jack (*Artocarpus integrifolia*), 8 - mango (*Mangifera indica*), 9 - maize (*Zea mays*), 10 - pepper (*Piper nigrum*), 11 - soya (*Glycine max*). Uncertainty bars correspond to one estimated standard deviation ($n = 10$, 8 pulses per test portion).

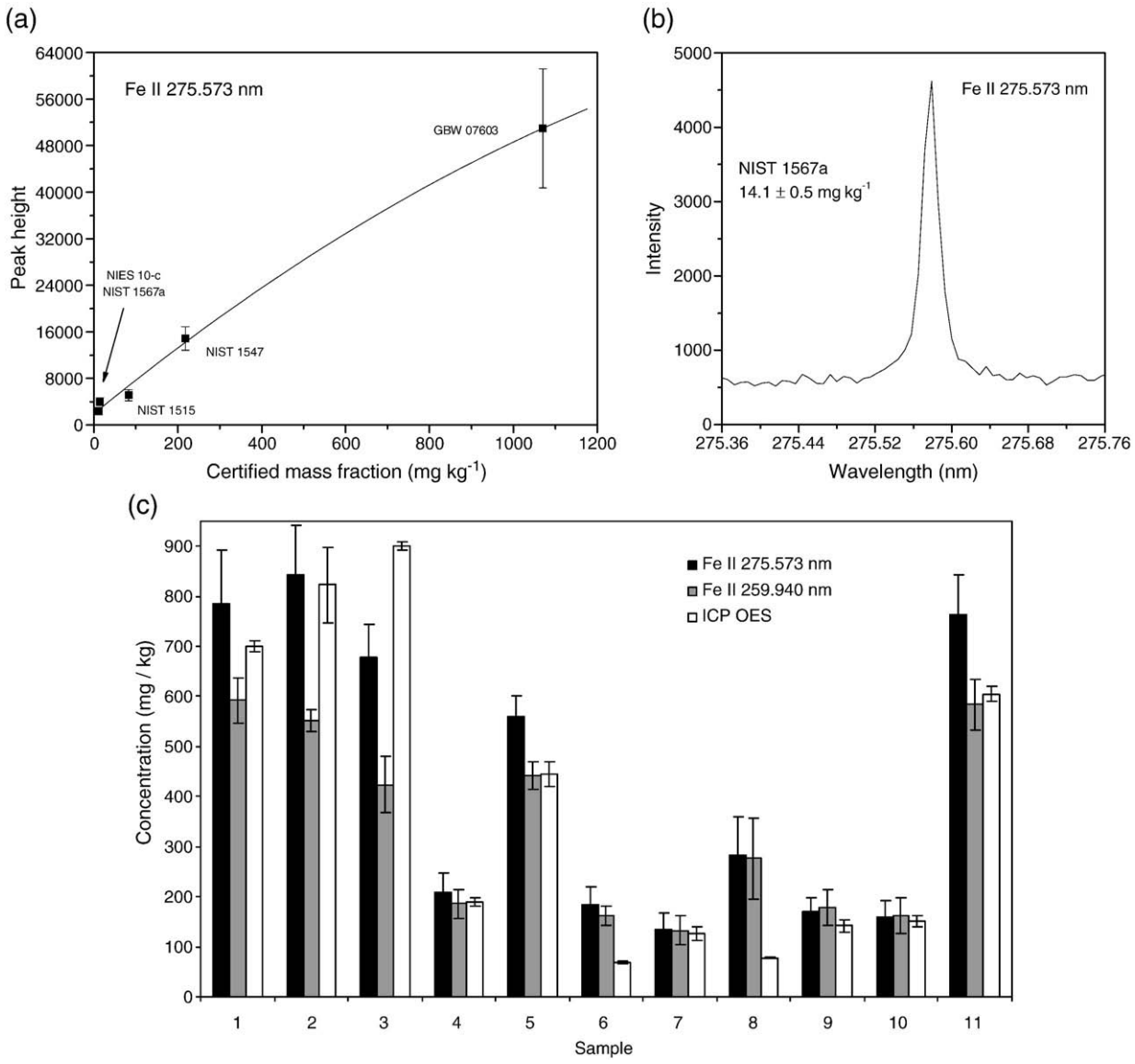

Fig. 3. (a) Analytical calibration curve for Fe II 259.940 nm using reference materials. (b) Signal profile for Fe II. (c) LIBS concentrations of Fe in plant samples compared to ICP OES results. Leave samples: 1 - lettuce (*Lactuca sativa*), 2 - endive (*Cichorium endivia*), 3 - boldo (*Pneumus boldus*), 4 - brachiaria (*Brachiaria decumbens*), 5 - coffee (*Coffea arabica*), 6 - grass (*Axonopus obtusifolius*), 7 - jack (*Artocarpus integrifolia*), 8 - mango (*Mangifera indica*), 9 - maize (*Zea mays*), 10 - pepper (*Piper nigrum*), 11 - soya (*Glycine max*). Uncertainty bars correspond to one estimated standard deviation ($n = 10$, 8 pulses per test portion).

that the main source of variation should be attributed to the inhomogeneity of the analytes microdistribution in the sample pellet, visual inspection of craters by using a stereoscopic microscope, showed significant variations in craters geometry among the different plant samples and among reference materials. For instance, the craters formed in spinach leaves (NIST 1570a) presented well defined walls and an uniform cylindrical shape, while craters formed in aquatic plant (BCR 60) pellets presented irregular shapes. So, another cause of uncertainty could be attributed to variations in the amount of vaporized mass from crater to crater. Although Hoffmann et al. [20] pointed out that this effect could also result from deviations in laser pulse energy, to variations in absorption coefficient from laser spot to laser spot, and to changes in the distance between the focal plane and the sample surface, in addition to changes in sample homogeneity, it should be addressed that particle size distribution is of key importance. As a sake of information, the uncertainties due to laser energy variation and counting statistics were less than 2% and 1%, respectively. In addition, the uncertainties of the certified properties of most reference materials used herein are lower than 2–4% at 95% confidence level, but it must be stressed that for test portions of at least 150 mg.

In this contribution, we are assuming that the main reasons for the relatively high coefficients of variation can be the micro-heterogeneity of the analytes in the pellets and the particle size distribution of the ground leaves for pellets preparation. As a pellet consists of grains of material of various sizes, the structure of particles packed together to form a pellet depends on the size distribution of the particles and on pellet porosity. The distribution of both composition and particle size can result in isolated volumes within the pellet where the local composition deviates from the overall average composition [21]. This effect can interfere in LIBS measurements when small sample masses are ablated. Rossbach and Zeiller [22] pointed out that final particle-size distribution is critical for the preparation of natural matrix reference materials suitable for microanalytical techniques. The materials should exhibit a low maximum ($\leq$50 μm) and a narrow range. Milling techniques to achieve such criteria must be employed.

As a result of variation in the material-laser interaction, strong pulse-to-pulse fluctuations of electronic excitation temperature and electron density were observed by Panne et al. [23]. These fluctuations can influence the relative intensities of single emission lines. By normalization of the line ratios via Saha-Boltzmann equilibrium

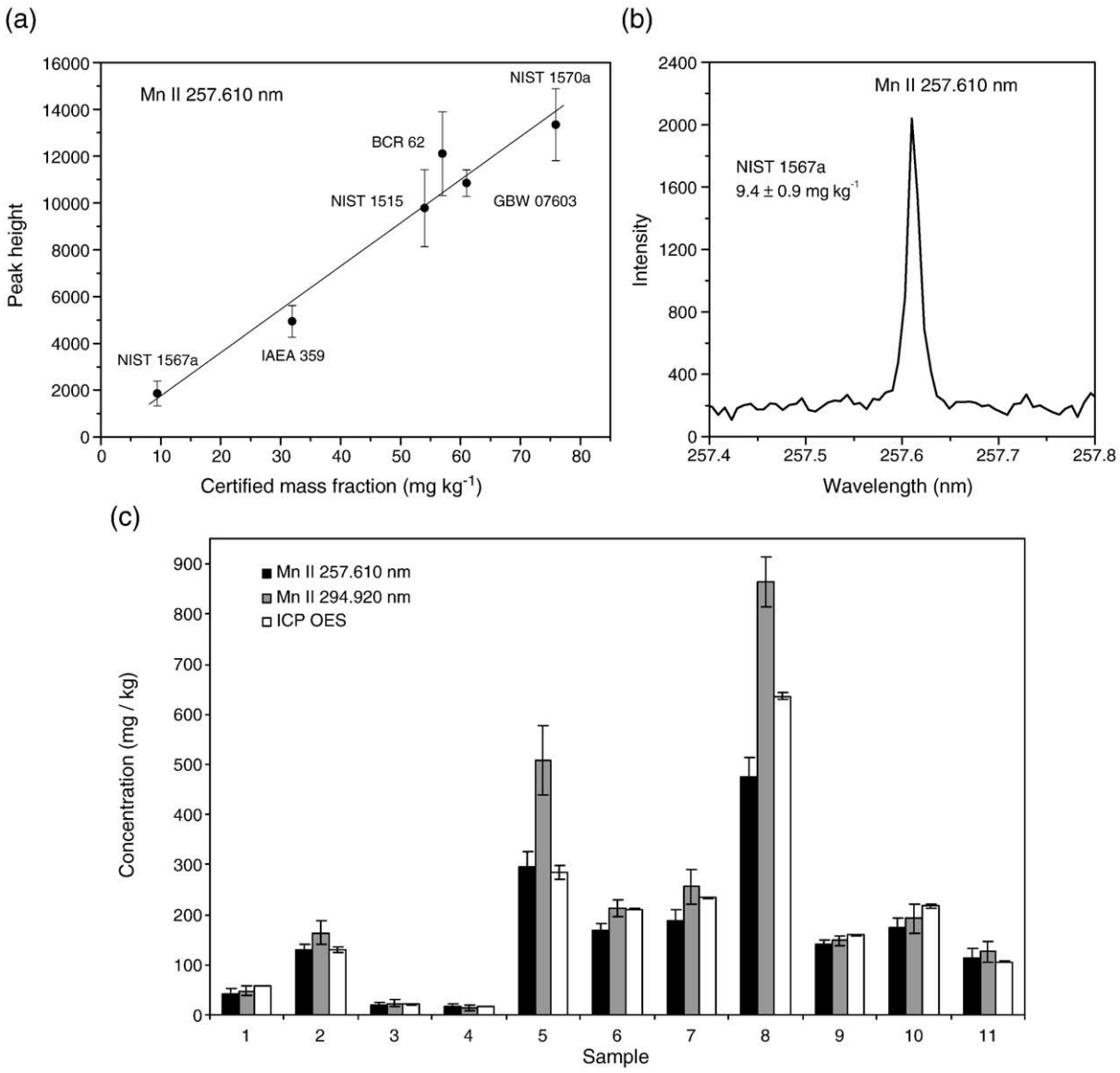

Fig. 4. (a) Analytical calibration curve for Mn II 257.610 nm. (b) Signal profile for Mn II. (c) LIBS concentrations of Mn in plant samples compared to ICP OES results. Leave samples: 1 - lettuce (*Lactuca sativa*), 2 - endive (*Cichorium endivia*), 3 - boldo (*Pneumus boldus*), 4 - brachiaria (*Brachiaria decumbens*), 5 - coffee (*Coffea arabica*), 6 - grass (*Axonopus obtusifolius*), 7 - jack (*Artocarpus integrifolia*), 8 - mango (*Mangifera indica*), 9 - maize (*Zea mays*), 10 - pepper (*Piper nigrum*), 11 - soya (*Glycine max*). Uncertainty bars correspond to one estimated standard deviation (n=10, 8 pulses per test portion).

relationships, the total variation of the line ratios can be reduced, improving coefficients of variation and accuracy for line ratios in LIBS. In this work, an attempt to improve the precision repeatability of the measurements was evaluated by using a carbon emission line intensity as internal standard in order to compensate for variation in the amount of the ablated sample mass. This approach is commonly applied in laser ablation inductively coupled mass spectrometry (LA-ICP-MS), where ^{13}C isotope is used for internal standardization for plant analysis [24]. For Ni determination in plant surfaces, ^{12}C was also employed [25]. As the spectrometer employed in this work has a wavelength range of 200 to 780 nm, C I line at 193.091 nm is not observed. A strong C I line was observed at 247.856 nm. However, this line can be interfered by Fe II 247.857 nm. In addition, C intensities were saturated in most spectra due to the high carbon content of plant material. So, in this contribution all the results were obtained without internal standardization. For future applications an attempt for data improvement, including C I 193.091 nm and data normalization, seems plausible.

Fig. 1b shows the peak profile for both B lines evaluated in this work. Line 249.773 nm was used for calibration (Fig. 1a) and for plant analysis. B I line at 249.677 nm was not well defined and presented high noise (Fig. 1b). The use of peak height and peak area for plant analysis, both with background subtraction, did not present significant differences (Fig. 1c). Therefore, peak height was used for concentration calculation in Figs. 2–5. Interferences caused by partial overlapping of analyte emission signals can be avoided or minimized by using peak height intensities. Results compared reasonably well with ICP OES data, except for coffee, jack, maize and pepper leaves, when LIBS concentrations were lower than ICP OES concentrations. These samples were also digested in TFM® vessels in a microwave oven and B contamination during digestion in hot plate was avoided.

Figs. 1a–5a show analytical calibration curves with linear fitting, except for Fe where a polyomial fitting was used. It is observed that B, Fe and Zn calibration curves did not pass through the origin. This effect was also observed by Sun et al. [18] for Al and Ca in NIST certified reference plant materials. As there were no blanks available for calibration, in principle, it was assumed that the analytical calibration curve should pass through the origin, unless there was a contamination during pellet preparation. A systematic error could be due, for example, to the iron present in the dial set made of stainless steel, but

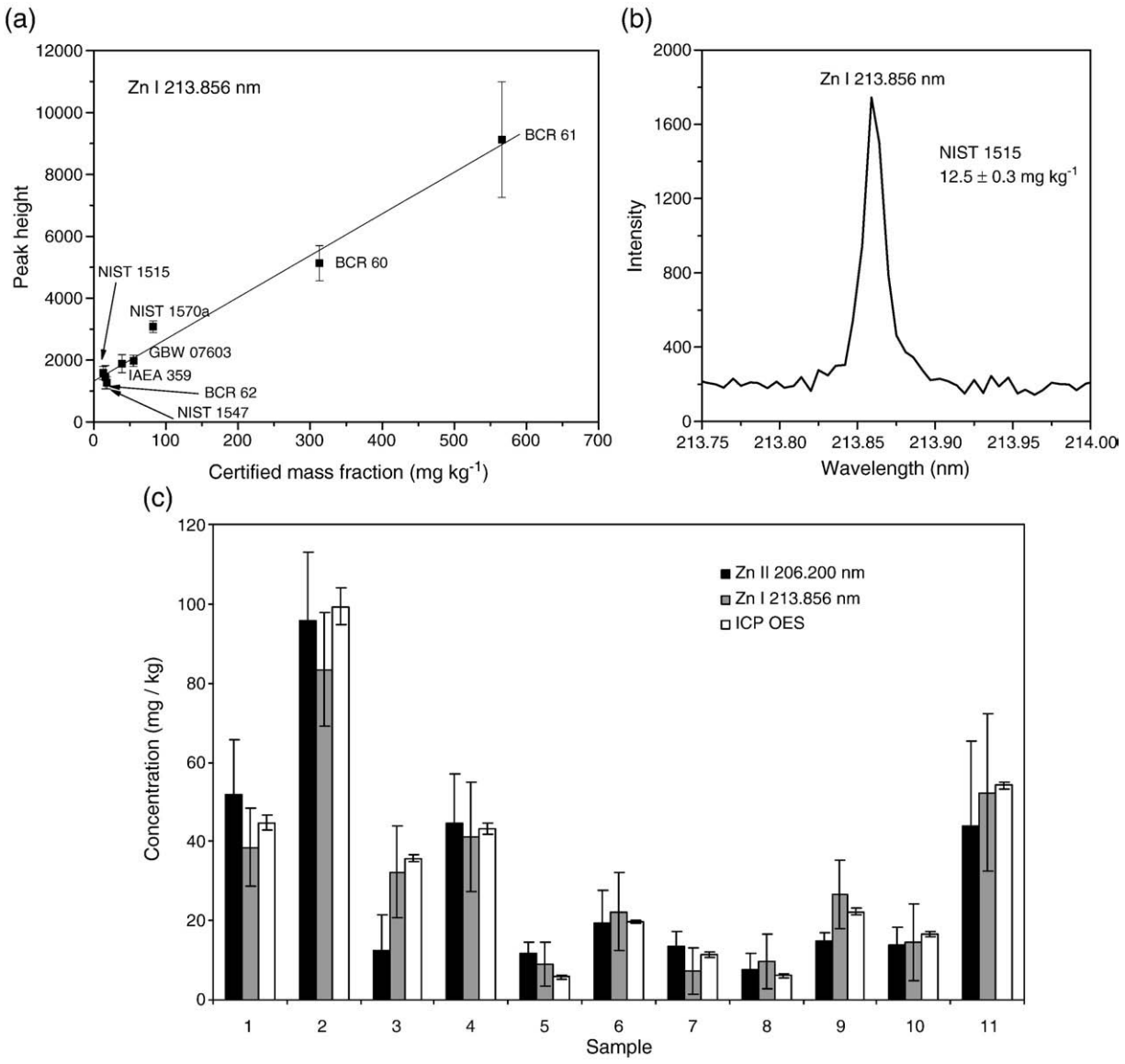

Fig. 5. (a) Analytical calibration curve for Zn I 213.859 nm using reference materials. (b) Signal profile for Zn I. (c) LIBS concentrations of Zn in plant samples compared to ICP OES results. Leave samples: 1 - lettuce (*Lactuca sativa*), 2 - endive (*Cichorium endivia*), 3 - boldo (*Pneumus boldus*), 4 - brachiaria (*Brachiaria decumbens*), 5 - coffee (*Coffea arabica*), 6 - grass (*Axonopus obtusifolius*), 7 - jack (*Artocarpus integrifolia*), 8 - mango (*Mangifera indica*), 9 - maize (*Zea mays*), 10 - pepper (*Piper nigrum*), 11 - soya (*Glycine max*). Uncertainty bars correspond to one estimated standard deviation ($n = 10$, 8 pulses per test portion).

this was not yet confirmed. Another explanation to the fact that the calibration curve could not pass through the origin can be attributed to self-absorption effects. For instance, Gornushkin et al. [26] observed an inflection in the calibration plot at the transition between an optically thin and an optically thick (self-absorption) plasma. This inflection depends on experimental conditions. If the conditions employed in this work led to an optically thick plasma, self-absorption effects could also contribute for the observed behavior in calibration curves. We have to stress that efforts must be done to address the best explanation for these phenomena.

Figs. 2c–5c show the results for Cu, Fe, Mn and Zn, respectively, with two wavelengths for each analyte. In most cases, the micronutrient concentrations measured by LIBS and ICP OES reasonably agree with at least at one of the wavelengths evaluated, mainly if uncertainties are taken into consideration. However, some exceptions could be observed. The results for Cu in endive, brachiaria, coffee, jack and mango leaves seemed to be overestimated by LIBS. Grass and mango leaves Fe concentrations were also overestimated by LIBS. On the other hand, for boldo leaves, Cu and Fe concentration was lower by LIBS than by ICP OES. Coffee and mango leaves presented the most discrepant results for Mn, B, Cu and Fe. It was not yet found a reason to explain for differences between LIBS and ICP OES results observed for these samples. Indeed, differences in craters diameter and depth were observed for different samples, even maintaining the 8 laser pulses in each crater, and it was probably caused by differences in the

Table 2
LIBS estimated limits of detection for B, Cu, Fe, Mn and Zn.

Element/wavelength (nm)	LOD (mg kg^{-1}) 8 pulses	LOD (mg kg^{-1}) 30 pulses
B I 249.773	2.2	1.4
Cu I 324.754	3.0	2.5
Cu I 327.396	5.0	4.0
Fe II 275.573	5.6	4.6
Fe II 259.940	3.6	2.8
Mn II 257.610	1.8	1.1
Mn II 294.920	5.5	4.2
Zn II 206.200	1.2	1.0
Zn I 213.856	3.2	2.9

Blank signals measured in the surroundings of each line. Data for Nd:YAG λ = 1064 nm, 200 mJ, 2 μs delay time, 5μs integration time.

Table 3
Comparison between LIBS results and Certified Reference values. Uncertainties of LIBS results represented by 2 estimated standard deviations ($n=10$).

Element	GBW 07603		NIST 1515		NIST 1547	
	LIBS (mg kg^{-1})	Certified (mg kg^{-1})	LIBS (mg kg^{-1})	Certified (mg kg^{-1})	LIBS (mg kg^{-1})	Certified (mg kg^{-1})
B	41 ± 6	38 ± 6	28 ± 8	27 ± 2	28 ± 9	29 ± 2
Cu	9 ± 2	6.6 ± 0.8	5 ± 2	5.64 ± 0.24	5 ± 1	3.7 ± 0.4
Fe	1010 ± 150	1070 ± 57	70 ± 20	83 ± 5	270 ± 50	218 ± 14
Mn	58 ± 6	61 ± 5	53 ± 18	54 ± 3	82 ± 18	98 ± 3
Zn	48 ± 9	55 ± 4	23 ± 6	12.5 ± 0.3	18 ± 6	17.9 ± 0.4

interaction of the laser beam with the pellets parent material from diverse plant samples.

The discrepant results could be attributed to matrix effects, i.e., the occurrence of various phenomena related to the strong influence of the material composition on the laser induced vaporization process and on subsequent plasma emission [27]. Eppler et al [28] monitored the emission signals of different compounds of Ba and Pb in a sand matrix and observed that analyte speciation can affect the slope of analytical calibration curves, reducing the accuracy of measurements for samples in which the exact speciation is unknown. The authors also observed analytical calibration curves with different slopes in soil and sand matrix. These matrix effects were related to differences in absorptivity, particle size distribution and elemental composition of the evaluated matrices. Due to these possible drawbacks, the calibration should be performed with standards having matrices similar to the one of the samples to be analysed [27]. On the other hand, the capability of LIBS to analyse quantitatively both bulk marbles and their surface encrustations has been demonstrated by correcting the results from calibration curves prepared with calcium carbonate matrices doped with certified soils. Suitable coefficients were calculated accounting the variability of the ablation rate, plasma temperature and electron density between samples and calibration curves [29]. Spectra normalization by integral emission significantly reduced the matrix influence on quantitative determination of Cr in soil and sediment samples [30].

Detection limits (Table 2) were estimated from the certified reference materials with the lowest mass fraction of each analyte in the calibration curve. As blank samples were not available, the estimated standard deviation of the background (s), measured in the surroundings of the selected emission line, was used ($n=10$) and detection limits were calculated as 3 s/b, where b is the angular coefficient of the calibration curve. Detection limits were appropriate for routine analysis of plant materials by using 8 pulses per test portion and varied, approximately, from 1.2 mg kg^{-1} Zn II at 206.200 nm to 5.6 mg kg^{-1} Fe II 275.573 nm. Detection limits were also calculated from results obtained with 30 pulses in each test portion, and up to 1.6 fold improvement was observed for B I 249.773 nm and Mn II 257.610 nm. When the ablation was made in the same sample position, a proportional increase in sensitivity was observed up to 4 pulses for all selected emission lines; after, the signal intensity did not increase proportionally with the number of shots, which is probably caused by changes in the sample surface geometry after 4 consecutive pulses. A significant improvement in the detection limit was not observed for Zn.

Trueness was also evaluated by randomly choosing one certified reference material from those mentioned herein and by using an analytical calibration curve made with a set of other CRMs. Results (Table 3) show that there was a reasonable agreement for most results, except for Zn in NIST 1515. It should be pointed out that uncertainties of LIBS results are represented by 2 times the estimated standard deviations. It is important to stress that validation is still necessary for each plant specie. Larger uncertainties in LIBS results were expected considering that the certified mass fractions were valid for test portions higher than 150 mg. The test portions ablated after 8 successive pulses represents approximately 360 μg, which is far bellow the recommended minimum sample mass in the certificates.

It is important to emphasize that strategies for improvement of coefficients of variation will be investigated. More appropriate LIBS sampling is expected if a large number of test portions are sampled, by using, for example, an ablation chamber that samples the test portions under continuous movement. At moment, an alternative set up was designed and is under evaluation in author's laboratory. In addition, sample presentation seems to be of key importance for improving the laser interaction with pellets prepared from powdered materials with similar particle size distribution.

4. Conclusions

Existing biological certified reference materials can be used for the preparation of pressed pellets in order to obtain LIBS calibration curves for the determination of Cu, Fe, Mn, Zn and B. The main difficulty is that the certified values are based on sample masses of at least 150 mg, which is much higher than the ablated test portion. As the test portion is quite small it is possible to see that the analyte is distributed heterogeneously in the sample pellet. The coefficient of variation of the results ($n=10$, 8 pulses per test portion) varied from 4 to 30% depending on the analyte and on the reference material.

The proposed procedure is very simple and acid digestion was avoided. Sample pellet is easily adapted in a compact ablation chamber. Measurements are made in each test portion in 1 s, and the number of test portions depends on sample micro-heterogeneity and lens-to-sample distance arrangement. In principle, at least 10 test portions per pellet are needed per analysis, but an increase in the number of test portions, for example to 100, will certainly lower the variance due to sampling in the pellet surface, and the sample throughput will be approximately 30 per hour.

Notwithstanding, it is clear that an effort must be done for the development of more appropriate certified reference materials for better calibration towards microanalysis of plant materials. Particle size distribution of CRM's and samples should also be taken into consideration. Even so, results indicate that LIBS can be an alternative to the already existing recommended methods that do require a sample decomposition step.

Improvements on sample presentation for LIBS analysis of plant materials is under investigation and includes evaluation of particle size distribution, pellet porosity, grinding procedures, binder addition and surface analysis by scanning electronic microscopy.

Acknowledgment

The authors are thankful to Fundação de Amparo à Pesquisa do Estado de São Paulo (FAPESP, Process: 04/15965-2, 06/06466-8, 05/50773-0) and to Conselho Nacional de Desenvolvimento Científico e Tecnológico (CNPq, Process: 477385/2006-0, 301285/2006-3) for financial support.

References

[1] K. Mengel, E.A. Kirkby, Principles of Plant Nutrition, 5th ed.Kluwer Academic Publishers, Netherlands, 2001.
[2] E. Malavolta, G.C. Vitti, S.A. Oliveira, Avaliação do Estado Nutricional das Plantas. Princípios e Aplicações, POTAFOS, Piracicaba, 1997.
[3] L.C. Trevizan, D. Santos Junior, R.E. Samad, N.D. Vieira Junior, C.S. Nomura, L.C. Nunes, I.A. Rufini, F.J. Krug, Evaluation of laser induced breakdown spectroscopy for the determination of macronutrients in plant materials, Spectrochim. Acta Part B 63 (2008) 1151–1158.
[4] O. Samek, D.C.S. Beddows, H.H. Telle, G.W. Morris, M. Liska, J. Kaiser, Quantitative analysis of trace metal accumulation in teeth using laser-induced breakdown spectroscopy, Appl. Phys. A 69 (1999) S179–S182.
[5] O. Samek, D.C.S. Beddows, H.H. Telle, J. Kaiser, M. Liska, J.O. Cáceres, A. Gonzáles Urena, Quantitative laser-induced breakdown spectroscopy analysis of calcified tissue samples, Spectrochim. Acta Part B 56 (2001) 865–875.
[6] Q. Sun, M. Tran, B.W. Smith, J.D. Winefordner, Zinc analysis in human skin by laser induced-breakdown spectroscopy, Talanta 52 (2000) 293–300.

[7] A. Assion, M. Wollenhaupt, L. Haag, F. Mayorov, C. Sarpe-Tudoran, M. Winter, U. Kutschera, T. Baumert, Femtosecond laser-induced-breakdown spectrometry for Ca^{2+} analysis of biological samples with high spatial resolution, Appl. Phys. B 77 (2003) 391–397.
[8] M. Corsi, G. Cristoforetti, M. Hidalgo, S. Legnaioli, V. Palleschi, A. Salvetti, E. Tognoni, C. Vallebona, Application of laser-induced breakdown spectroscopy technique to hair tissue mineral analysis, Appl. Opt. 42 (2003) 6133–6137.
[9] A. Kumar, F.Y. Yueh, J.P. Singh, S. Burgess, Characterization of malignant tissue cells by laser-induced breakdown spectroscopy, Appl. Opt. 43 (2004) 5399–5403.
[10] M. Baudelet, L. Guyon, J. Yu, J.P. Wolf, T. Amodeo, E. Fréjafon, Femtosecond time-resolved laser-induced breakdown spectroscopy for detection and identification of bacteria: a comparison to the nanosecond regime, J. Appl. Phys. 99 (2006) 084701.
[11] A.A. Oraevsky, L.B. Da Silva, A.M. Rubenchik, M.D. Feit, M.E. Glinsky, M.D. Perry, B.M. Mammini, W. Small, B.C. Stuart, Plasma mediated ablation of biological tissues with nanosecond-to-femtosecond laser pulses: relative role of linear and nonlinear absorption, IEEE J. Sel. Top. Quantum Electron. 2 (1996) 801–809.
[12] O. Samek, J. Lambert, R. Hergenröder, M. Liska, J. Kaiser, K. Novotny, S. Kukhlevsky, Femtosecond laser spectrochemical analysis of plant samples, Laser Phys. Lett. 3 (2006) 21–25.
[13] J. Kaiser, O. Samek, L. Reale, M. Liska, R. Malina, A. Ritucci, A. Poma, A. Tucci, F. Flora, A. Lai, L. Mancini, G. Tromba, F. Zanini, A. Faenov, T. Pikuz, G. Cinque, Monitoring of the heavy-metal hyperaccumulation in vegetal tissues by X-ray radiography and by femto-second laser induced breakdown spectroscopy, Microsc. Res. Tech. 70 (2007) 147–153.
[14] M. Galiová, J. Kaiser, K. Novotny, O. Samek, L. Reale, R. Malina, K. Páleníková, M. Liska, V. Cudek, V. Kanicky, V. Otruba, A. Poma, A. Tucci, Utilization of laser induced breakdown spectroscopy for investigation of the metal accumulation in vegetal tissues, Spectrochim. Acta Part B 62 (2007) 1597–1605.
[15] V. Juvé, R. Portelli, M. Boueri, M. Baudelet, J. Yu, Space-resolved analysis of trace elements in fresh vegetables using ultraviolet nanosecond laser-induced breakdown spectroscopy, Spectrochim. Acta Part B 63 (2008) 1047–1053.
[16] J. Kaiser, M. Galiová, K. Novotny, R. Cervenka, L. Reale, J. Novotny, M. Liska, O. Samek, V. Kanicky, A. Hrdlicka, K. Stejskal, V. Adam, R. Kizek, Mapping of lead, magnesium and cupper accumulation in plant tissues by laser-induced breakdown spectroscopy and laser-ablation inductively coupled plasma mass spectrometry, Spectrochim. Acta Part B 64 (2008) 67–73.
[17] D. Santos Jr., R.E. Samad, L.C. Trevizan, A.Z. Freitas, N.D. Vieira Jr., F.J. Krug, Evaluation of femtosecond laser-induced breakdown spectroscopy for analysis of animal tissues, Appl. Spectrosc. 62 (2008) 1137–1143.
[18] Q. Sun, M. Tran, B.W. Smith, J.D. Winefordner, Direct determination of P, Al, Ca, Cu, Mn, Zn, Mg and Fe in plant materials by laser-induced plasma spectroscopy, Can. J. Anal. Sci. Spectrosc. 44 (1999) 164–170.
[19] V.I. Babushok, F.C. DeLucia Jr., P.J. Dagdigian, A.W. Miziolek, Experimental and kinetic modeling study of the laser-induced breakdown spectroscopy plume from metallic lead in argon, Spectrochim. Acta Part B 60 (2005) 926–934.
[20] E. Hoffmann, C. Lüdke, H. Scholze, Is laser-ablation-ICP-MS and alternative to solution analysis of solid samples? Fresenius J. Anal. Chem. 359 (1997) 394–398.
[21] G.A. Georgalli, M.A. Reuter, A particle packing algorithm for pellet design with a predetermined size distribution, Powder Technol. 173 (2007) 189–199.
[22] M. Rossbach, E. Zeiller, Assessment of element-specific homogeneity in reference materials using microanalytical techniques, Anal. Bioanal. Chem. 377 (2003) 334–339.
[23] U. Panne, C. Haisch, M. Clara, R. Niessner, Analysis of glass and glass melts during the vitrification process of fly and bottom ashes by laser-induced plasma spectroscopy. Part I: normalization and plasma diagnostic, Spectrochim. Acta Part B 53 (1998) 1957–1968.
[24] E. Hoffmann, C. Lüdke, J. Skole, H. Stephanowitz, E. Ullrich, D. Colditz, Spatial determination of elements in green leaves of oak trees (*Quercus robur*) by laser ablation-ICP-MS, Fresenius J. Anal. Chem. 367 (2000) 579–585.
[25] T. Punshon, B.P. Jackson, P.M. Bertsch, J. Burger, Mass loading of nickel and uranium on plant surfaces: application of laser ablation-ICP-MS, J. Environ. Monit. 6 (2004) 153–159.
[26] I.B. Gornushkin, J.M. Anzano, L.A. King, B.W. Smith, N. Omenetto, J.D. Winefordner, Curve of growth methodology applied to laser-induced plasma emission spectroscopy, Spectrochim. Acta Part B 54 (1999) 491–503.
[27] R. Fantoni, L. Caneve, F. Colao, L. Fornarini, V. Lazic, V. Spizzichino, Methodologies for laboratory laser induced breakdown spectroscopy semi-quantitative and quantitative analysis — a review, Spectrochim. Acta Part B 63 (2008) 1097–1108.
[28] A.S. Eppler, D.A. Cremers, D.D. Hickmott, M.J. Ferris, A.C. Koskelo, Matrix effects in the detection of Pb and Ba in soils using laser-induced breakdown spectroscopy, Appl. Spectrosc. 50 (1996) 1175–1181.
[29] V. Lazic, R. Fantoni, F. Colao, A. Santagata, A. Morone, V. Spizzichino, Quantitative laser induced breakdown spectroscopy analysis of ancient marble and corrections for the variability of plasma parameters and of ablation rate, J. Anal. At. Spectrom. 19 (2004) 429–436.
[30] V. Lazic, R. Barbini, F. Colao, R. Fantoni, A. Palucci, Self-absorption model in quantitative laser induced breakdown spectroscopy measurements on soils and sediments, Spectrochim. Acta Part B 56 (2000) 807–820.